Supporting Information

Solvent-Modulated Luminescent Spheroidal Assemblies of Cu_8 Nanocluster for Volatile Amine Sensing

Subrata Duary,[a] Arijit Jana,[a] Amitabha Das,[b] Ankit Sharma,[c] Biswarup Pathak,*[b] Kumaran Nair Valsala Devi Adarsh,*[c] and Thalappil Pradeep*[a]

Authors affiliations

[a] DST Unit of Nanoscience (DST UNS) and Thematic Unit of Excellence (TUE), Department of Chemistry, Indian Institute of Technology Madras, Chennai – 600036, India.

*E-mail: pradeep@iitm.ac.in

[b] Department of Chemistry, Indian Institute of Technology Indore, Indore 453552, India.

*E-mail: biswarup@iiti.ac.in

[c] Department of Physics, Indian Institute of Science Education and Research Bhopal, Bhopal 462066, India.

*E-mail: adarsh@iiserb.ac.in

Table of contents

Experimental set up for visual detection of volatile amine sensing, emphasizing on foodstuffs (fish and chicken) spoilage monitoring.

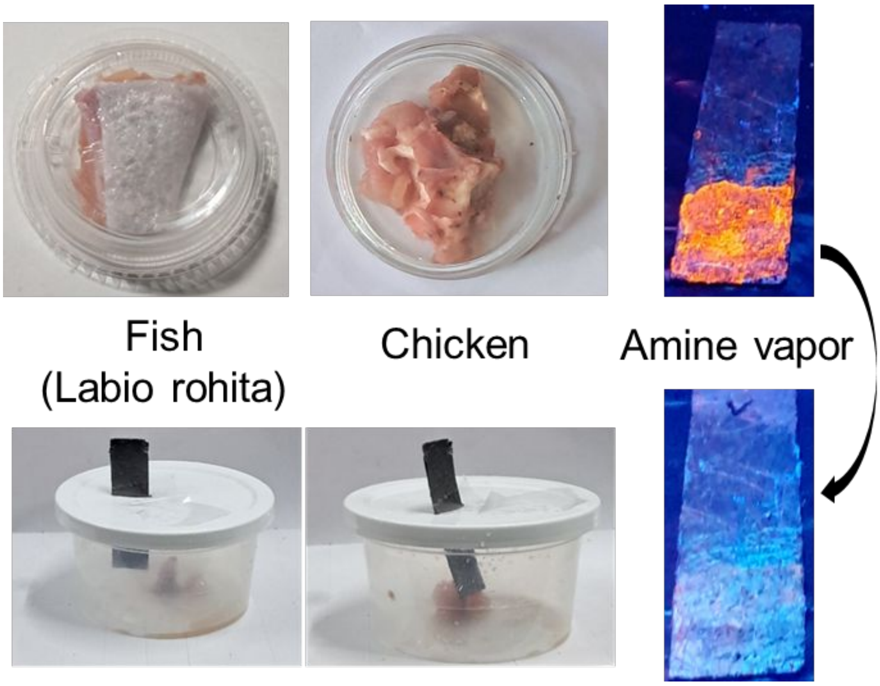

Table S1. Crystal data and structure refinement for Cu_8 NC.

Identification code	Cu_8 SM	
Empirical formula	$C_{130}H_{114}Cu_8F_{12}N_{10}O_6P_8S_4$	
Formula weight	3024.63	
Temperature	200(2) K	
Wavelength	1.54178 Å	
Crystal system	Triclinic	
Space group	P -1	
Unit cell dimensions	a = 16.7932(9) Å	a= 94.644(2)°.
	b = 16.9244(9) Å	b= 97.173(2)°.
	c = 26.2178(14) Å	g = 116.938(2)°.
Volume	6510.8(6) $Å^3$	
Z	2	
Density (calculated)	1.543 Mg/m^3	
Absorption coefficient	3.562 mm^{-1}	
F(000)	3072	
Crystal size	0.181 x 0.132 x 0.032 mm^3	
Theta range for data collection	1.719 to 68.482°.	
Index ranges	-20<=h<=20, -20<=k<=20, -30<=l<=31	

Reflections collected	226915
Independent reflections	23900 [R(int) = 0.0825]
Completeness to theta = 67.679°	99.9 %
Absorption correction	Semi-empirical from equivalents
Max. and min. transmission	0.6695 and 0.4908
Refinement method	Full-matrix least-squares on F^2
Data / restraints / parameters	23900 / 31 / 1604
Goodness-of-fit on F^2	1.059
Final R indices [I>2sigma(I)]	R1 = 0.0534, wR2 = 0.1376
R indices (all data)	R1 = 0.0728, wR2 = 0.1594
Extinction coefficient	0.00067(5)
Largest diff. peak and hole	0.518 and -0.562 e.Å^{-3}

Table S2. Atomic coordinates (x 10^4) and equivalent isotropic displacement parameters (Å^{2}x 10^3) for Cu_8 NC. U(eq) is defined as one third of the trace of the orthogonalized U^{ij} tensor.

	x	y	z	U(eq)
Cu(1)	5878(1)	4273(1)	7592(1)	57(1)
Cu(2)	5981(1)	3032(1)	8074(1)	57(1)
Cu(3)	6734(1)	3089(1)	7270(1)	57(1)
Cu(4)	5088(1)	2802(1)	6942(1)	58(1)
Cu(5)	6737(1)	5751(1)	8369(1)	61(1)
Cu(6)	6148(1)	1602(1)	8493(1)	63(1)
Cu(7)	7364(1)	3120(1)	6358(1)	63(1)
Cu(8)	3327(1)	2642(1)	6689(1)	66(1)
C(1)	7239(3)	3328(3)	4960(2)	71(1)
C(2)	6759(5)	3802(5)	5006(3)	107(2)
C(3)	6354(6)	3969(6)	4566(3)	131(3)
C(4)	6409(5)	3656(6)	4083(3)	117(2)
C(5)	6910(5)	3218(4)	4028(2)	99(2)
C(6)	7321(4)	3050(4)	4465(2)	83(1)
C(7)	8955(3)	3658(3)	5526(2)	71(1)
C(8)	9478(4)	4491(4)	5819(2)	90(2)

C(9)	10392(4)	4983(5)	5798(3)	105(2)
C(10)	10788(4)	4640(5)	5495(3)	103(2)
C(11)	10299(4)	3811(5)	5205(3)	106(2)
C(12)	9380(4)	3317(4)	5218(2)	90(2)
C(13)	7399(3)	1890(3)	5372(2)	71(1)
C(14)	7683(3)	1534(3)	5837(2)	72(1)
C(15)	6058(3)	782(3)	6241(2)	71(1)
C(16)	5358(4)	969(4)	6117(3)	94(2)
C(17)	4479(4)	296(5)	5948(3)	114(2)
C(18)	4286(5)	-569(5)	5918(3)	105(2)
C(19)	4980(5)	-783(4)	6040(3)	115(2)
C(20)	5874(4)	-102(4)	6207(3)	102(2)
C(21)	7895(3)	1548(3)	6925(2)	69(1)
C(22)	7602(4)	846(4)	7209(2)	87(2)
C(23)	8213(5)	764(5)	7575(3)	106(2)
C(24)	9107(4)	1377(5)	7676(2)	99(2)
C(25)	9400(4)	2091(4)	7419(2)	90(2)
C(26)	8801(4)	2187(4)	7045(2)	80(1)
C(27)	6233(3)	-547(3)	8139(2)	72(1)
C(28)	5652(4)	-765(3)	7675(2)	81(1)
C(29)	5558(5)	-1438(4)	7296(3)	103(2)
C(30)	6060(5)	-1883(4)	7383(3)	108(2)
C(31)	6624(5)	-1686(4)	7836(3)	104(2)
C(32)	6734(4)	-1018(4)	8221(2)	88(2)
C(33)	5700(3)	-327(3)	9097(2)	72(1)
C(34)	4891(5)	-366(5)	9156(3)	120(3)
C(35)	4376(6)	-907(7)	9484(4)	168(4)
C(36)	4697(6)	-1362(5)	9777(4)	133(3)
C(37)	5489(6)	-1336(4)	9725(3)	109(2)
C(38)	5994(5)	-828(4)	9385(2)	92(2)
C(39)	7509(3)	876(3)	8953(2)	73(1)
C(40)	7704(3)	1637(3)	9372(2)	74(1)
C(41)	7302(3)	3047(3)	9713(2)	68(1)
C(42)	6828(4)	3525(4)	9676(2)	93(2)
C(43)	6766(5)	3992(6)	10114(3)	120(2)
C(44)	7164(5)	3965(5)	10594(3)	115(2)
C(45)	7630(5)	3489(5)	10644(2)	101(2)
C(46)	7708(4)	3043(4)	10207(2)	86(2)

C(47)	8429(3)	3309(3)	8954(2)	60(1)
C(48)	8649(4)	3140(4)	8480(2)	75(1)
C(49)	9457(4)	3755(4)	8348(2)	83(1)
C(50)	10035(4)	4528(4)	8677(2)	84(1)
C(51)	9807(4)	4703(4)	9142(2)	83(1)
C(52)	9014(3)	4105(3)	9282(2)	74(1)
C(53)	8417(3)	8067(3)	8753(2)	73(1)
C(54)	8770(4)	7991(4)	8312(2)	93(2)
C(55)	9310(4)	8737(6)	8109(3)	116(2)
C(56)	9497(5)	9573(6)	8352(4)	137(3)
C(57)	9164(5)	9664(5)	8788(4)	127(3)
C(58)	8619(4)	8911(4)	8988(3)	98(2)
C(59)	8331(3)	7010(3)	9568(2)	67(1)
C(60)	8572(4)	7609(4)	10024(2)	81(1)
C(61)	9089(4)	7553(4)	10464(2)	92(2)
C(62)	9369(5)	6918(5)	10448(3)	107(2)
C(63)	9147(6)	6334(5)	10000(3)	130(3)
C(64)	8627(5)	6374(4)	9563(2)	102(2)
C(65)	6812(3)	7310(3)	9201(2)	67(1)
C(66)	6008(3)	6449(3)	9276(2)	67(1)
C(67)	4782(3)	6066(3)	8303(2)	64(1)
C(68)	4645(4)	6767(4)	8501(2)	85(2)
C(69)	4106(4)	7043(4)	8199(3)	102(2)
C(70)	3683(4)	6608(4)	7702(3)	96(2)
C(71)	3805(5)	5907(5)	7507(2)	103(2)
C(72)	4358(4)	5649(4)	7801(2)	85(2)
C(73)	4685(3)	4676(3)	8903(2)	63(1)
C(74)	3790(3)	4475(4)	8908(2)	88(2)
C(75)	3242(4)	3747(5)	9130(3)	107(2)
C(76)	3571(4)	3212(4)	9339(2)	91(2)
C(77)	4444(4)	3402(4)	9332(2)	91(2)
C(78)	4997(4)	4121(4)	9112(2)	81(1)
C(79)	3487(4)	2642(3)	5371(2)	80(1)
C(80)	2843(4)	2441(4)	4929(2)	97(2)
C(81)	2803(6)	1909(6)	4491(3)	127(3)
C(82)	3381(9)	1578(7)	4486(3)	164(4)
C(83)	4026(9)	1750(8)	4913(4)	190(5)
C(84)	4062(6)	2284(6)	5358(3)	130(3)

C(85)	4519(3)	4393(3)	5999(2)	71(1)
C(86)	4698(4)	4996(4)	6439(2)	87(2)
C(87)	5384(5)	5855(4)	6502(3)	113(2)
C(88)	5908(5)	6118(5)	6133(4)	125(3)
C(89)	5768(5)	5520(6)	5703(3)	117(2)
C(90)	5070(4)	4642(4)	5629(2)	87(2)
C(91)	2586(4)	3537(4)	5847(2)	80(1)
C(92)	1724(3)	2735(4)	5924(2)	80(1)
C(93)	1208(5)	3753(5)	6780(3)	98(2)
C(94)	1087(5)	4362(5)	7096(3)	115(2)
C(95)	1395(5)	4523(5)	7609(3)	109(2)
C(96)	1838(4)	4077(5)	7827(3)	108(2)
C(97)	1991(4)	3487(4)	7513(2)	90(2)
C(98)	1677(3)	3315(4)	6981(2)	76(1)
C(99)	880(4)	1423(4)	6577(2)	81(1)
C(100)	998(5)	756(5)	6771(3)	129(3)
C(101)	259(6)	-78(6)	6776(4)	155(4)
C(102)	-593(5)	-221(6)	6584(3)	128(3)
C(103)	-717(5)	429(5)	6382(4)	130(3)
C(104)	8(4)	1256(5)	6377(3)	109(2)
C(105)	4880(3)	1164(3)	7352(2)	57(1)
C(106)	3586(3)	-109(3)	7315(2)	79(1)
C(107)	3098(3)	174(3)	7005(2)	77(1)
C(108)	3554(3)	1034(3)	6856(2)	64(1)
C(109)	3132(4)	-1007(5)	7493(4)	128(3)
C(110)	4046(3)	2599(3)	7903(2)	56(1)
C(111)	4434(3)	1782(3)	8475(2)	62(1)
C(112)	3501(3)	1328(3)	8513(2)	74(1)
C(113)	2928(3)	1572(3)	8243(2)	72(1)
C(114)	1941(4)	1123(5)	8277(3)	101(2)
C(115)	6793(3)	4666(3)	6685(2)	56(1)
C(116)	7100(3)	5927(3)	7276(2)	59(1)
C(117)	7758(3)	6444(3)	6985(2)	66(1)
C(118)	7864(3)	6011(3)	6562(2)	67(1)
C(119)	8555(4)	6518(4)	6236(3)	90(2)
C(120)	7954(3)	4779(3)	7987(2)	56(1)
C(121)	8578(3)	4477(3)	7291(2)	58(1)
C(122)	9373(3)	5292(3)	7495(2)	67(1)

C(123)	9378(3)	5771(3)	7934(2)	66(1)
C(124)	10221(4)	6638(4)	8172(3)	90(2)
O(1)	8504(2)	4001(2)	6876(1)	69(1)
O(2)	6947(2)	6262(2)	7675(1)	69(1)
O(3)	5012(2)	1596(2)	8716(1)	72(1)
O(4)	3151(2)	1356(2)	6572(1)	74(1)
S(1)	7004(1)	4480(1)	8308(1)	55(1)
S(2)	6065(1)	1821(1)	7610(1)	56(1)
S(3)	4375(1)	3402(1)	7469(1)	57(1)
S(4)	6198(1)	3485(1)	6492(1)	56(1)
P(1)	7745(1)	3092(1)	5546(1)	64(1)
P(2)	7201(1)	1727(1)	6401(1)	64(1)
P(3)	6309(1)	329(1)	8626(1)	65(1)
P(4)	7382(1)	2471(1)	9120(1)	62(1)
P(5)	7666(1)	7036(1)	8971(1)	62(1)
P(6)	5484(1)	5658(1)	8664(1)	59(1)
P(7)	3562(1)	3296(1)	5969(1)	67(1)
P(8)	1879(1)	2501(1)	6594(1)	72(1)
N(1)	8678(2)	5557(2)	8190(1)	63(1)
N(2)	7873(2)	4218(2)	7566(1)	54(1)
N(3)	6625(2)	5019(2)	7112(1)	55(1)
N(4)	7398(2)	5118(2)	6395(1)	63(1)
N(5)	4483(3)	364(2)	7497(2)	71(1)
N(6)	4476(2)	1519(2)	7043(1)	57(1)
N(7)	4691(2)	2447(2)	8169(1)	57(1)
N(8)	3173(2)	2200(3)	7925(2)	66(1)
F(1)	8902(4)	7385(3)	6360(2)	176(2)
F(2)	8202(4)	6346(4)	5742(2)	164(2)
F(3)	9211(3)	6325(3)	6257(2)	154(2)
F(4)	1504(3)	376(4)	7972(3)	204(3)
F(5)	1786(3)	910(5)	8732(2)	190(3)
F(6)	1518(3)	1556(4)	8163(3)	185(3)
F(7)	3395(4)	-1568(3)	7270(3)	203(3)
F(8)	2266(3)	-1424(3)	7349(3)	199(3)
F(9)	3353(4)	-1003(4)	7969(3)	216(4)
F(10)	10963(2)	6659(3)	8060(2)	152(2)
F(11)	10362(3)	6760(3)	8684(2)	156(2)
F(12)	10191(3)	7332(2)	8032(2)	156(2)

C(125)	1912(8)	-1054(7)	9055(5)	193(5)
C(126)	747(8)	-1182(12)	9510(6)	263(9)
C(127)	2161(10)	159(7)	9670(4)	195(6)
N(9)	1609(6)	-651(5)	9453(3)	140(3)
O(5)	2136(5)	679(5)	9940(3)	187(3)
O(6)	1704(11)	-1468(6)	5775(5)	276(6)
N(10)	1120(6)	-649(6)	5476(3)	159(3)
C(129)	1395(11)	273(9)	5383(7)	346(12)
C(128)	1861(10)	-760(10)	5676(6)	250(8)
C(130)	215(9)	-1277(10)	5337(7)	289(9)

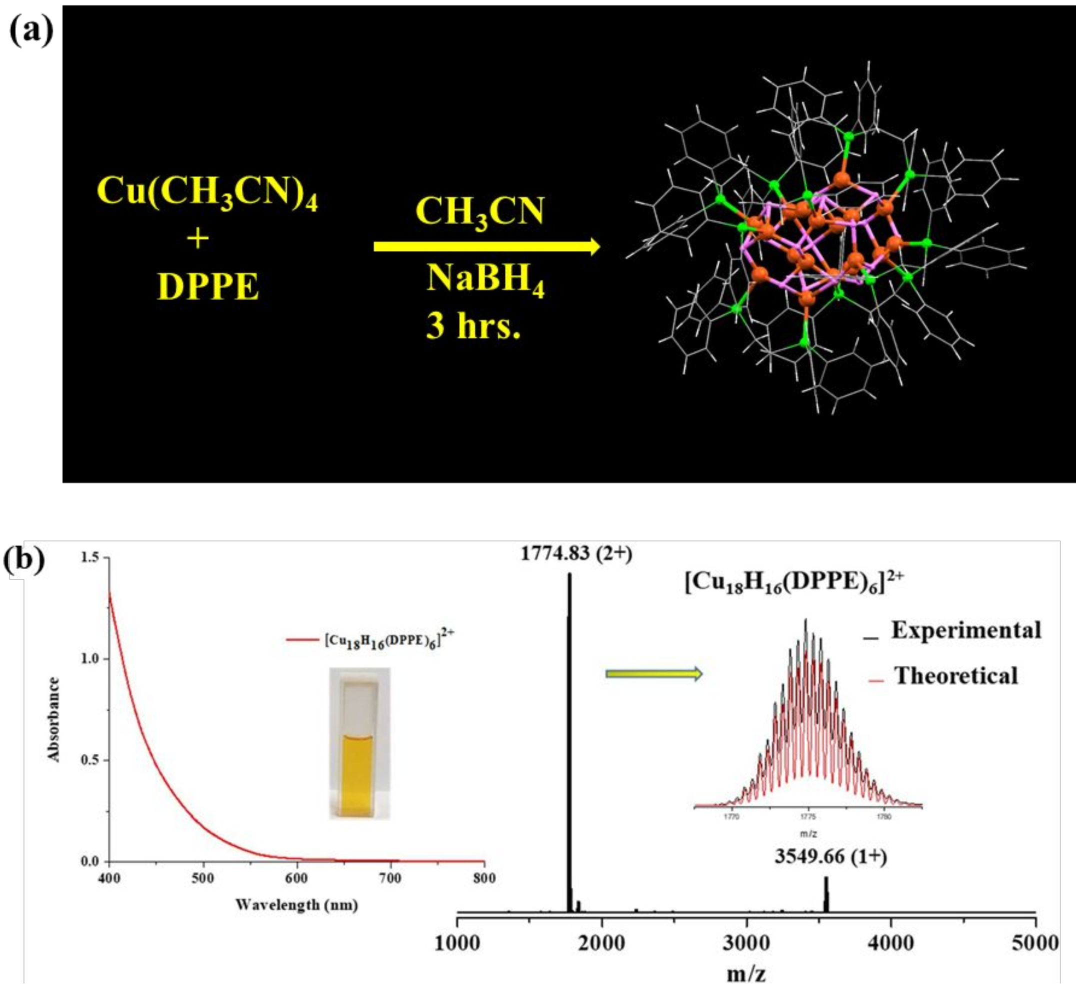

Figure S1. (a) Scheme for synthesis of Cu_{18} NC. (b) UV-vis. and ESI MS spectra of as synthesized Cu_{18} NC Atomic color code: orange=Cu, yellow=S, green=P, grey=C, red=O, blue=N, F= light green and white/magenta=H.

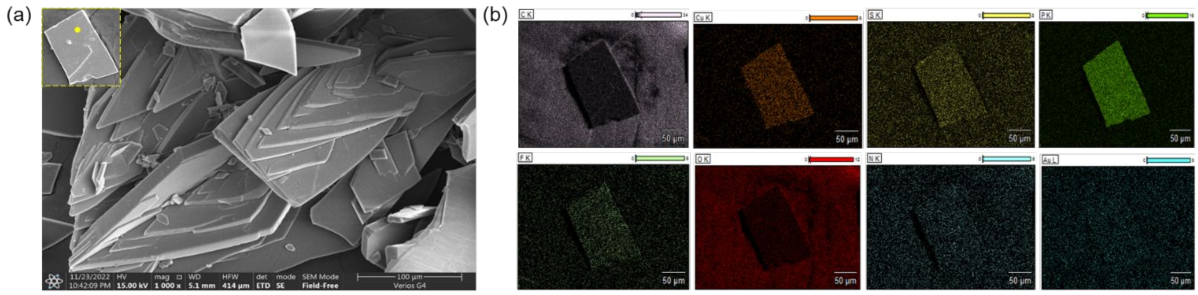

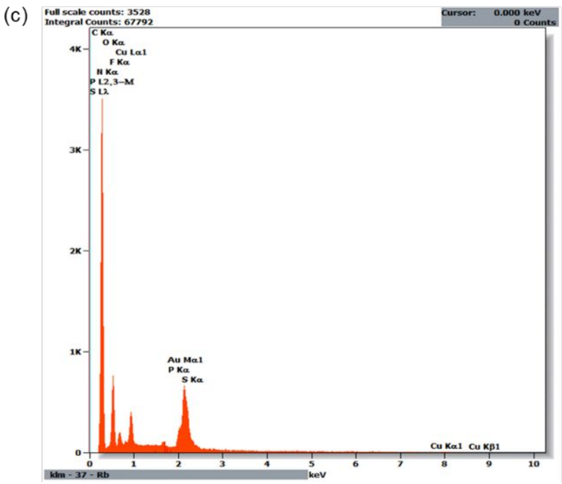

(d)

Element	Weight %	Atom %
C K	44.93	67.13
Cu K	5.69	1.61
S K	0.10	0.06
P K	2.13	1.23
F K	0.30	0.28
O K	20.23	22.69
N K	3.84	4.92
Au M	22.78	2.08

Figure S2. (a) FESEM images of agglomerated sheets of single crystals. (b) EDS mapping of each elements. (c) EDS spectra. (d) Weight and atomic percentage of elements from FESEM analysis.

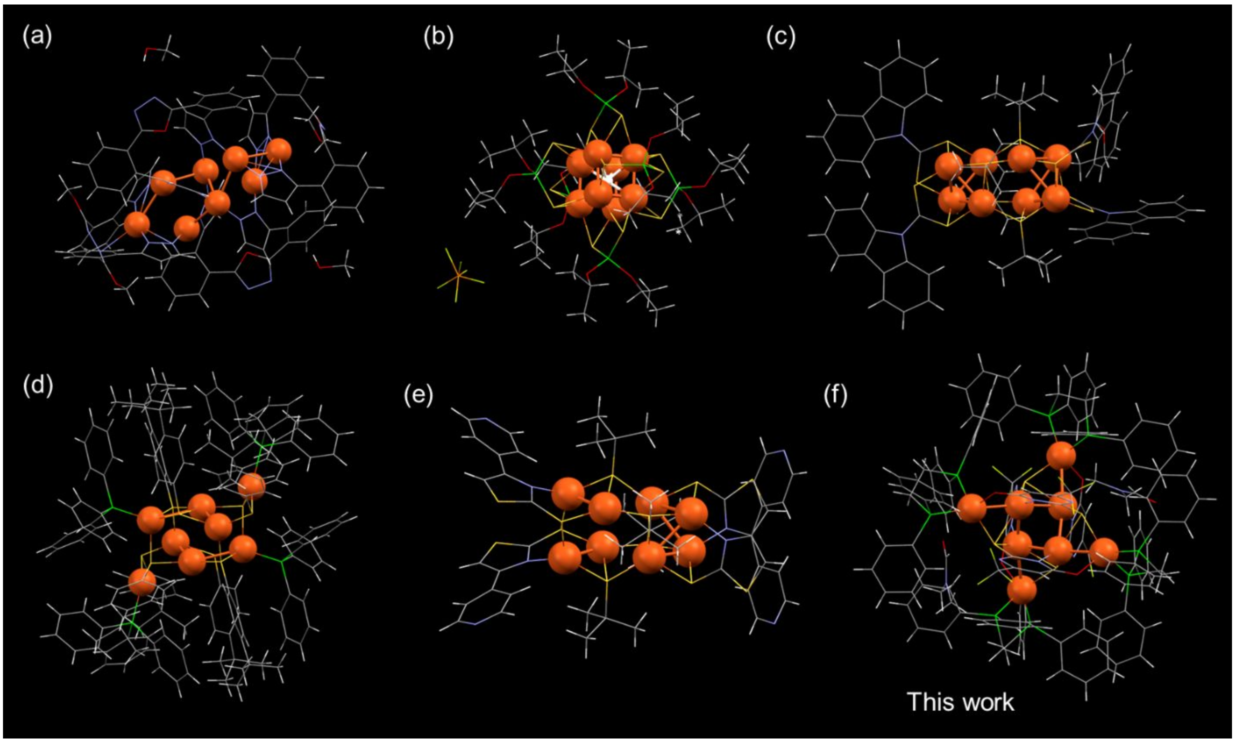

Figure S3. A comparison between single crystal structure of reported Cu_8 clusters, such as (a) puckered core [1] (b) cubic structure [2] (c) two fused tetrahedron [3], (d) bi-capped octahedral, [4] (e) one tetrahedral stapled by two Cu_2 unit [5] along with tetrahedral Cu_4 unit and (f) tetra capped distorted square planner structure. Atomic color code: orange=Cu, yellow=S, green=P, grey=C, red=O, blue=N, F= light green and white=H.

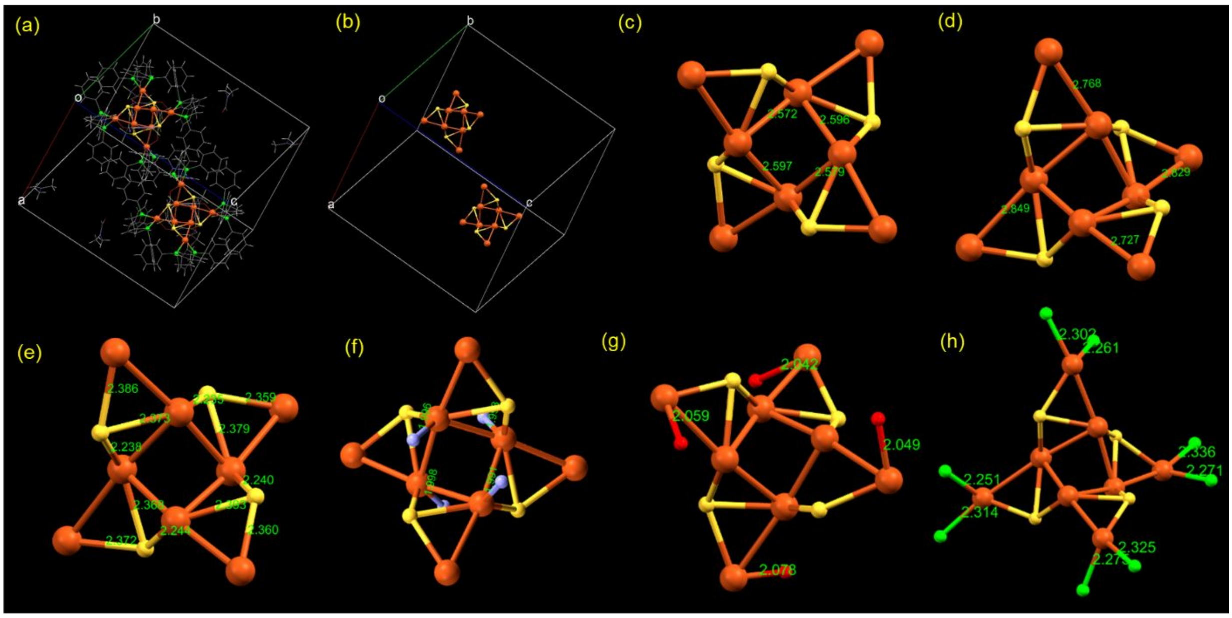

Figure S4. (a,b) Complete structure and core of clusters per unit cell. (c,d,e,f,g,h) bond distances of inner Cu-Cu, outer Cu-Cu, Cu-S, Cu-N, Cu-O and Cu-P respectively. Atomic color code: orange=Cu, yellow=S, green=P, grey=C, red=O, blue=N, F= light green and white=H.

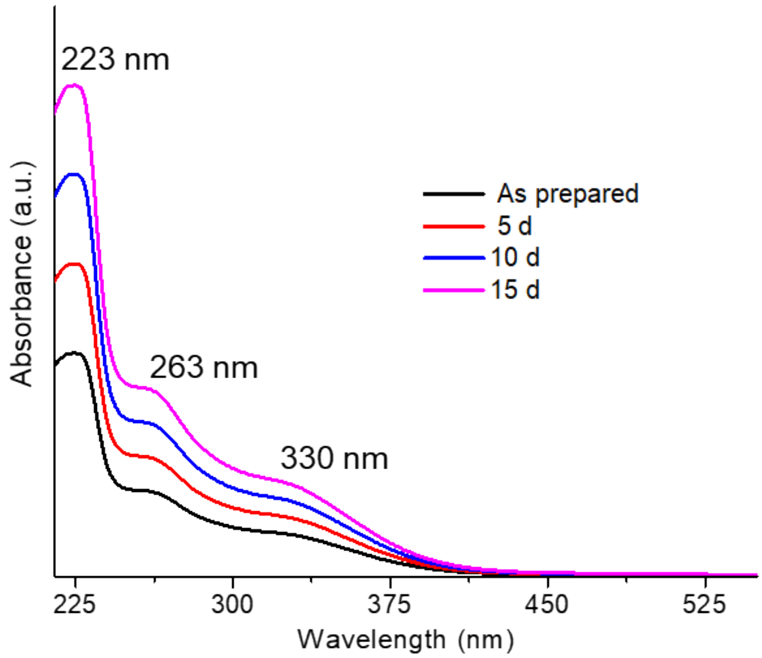

Figure S5. UV-vis. spectra of Cu_8 NC dissolved in acetonitrile indicating stability up to 15 days.

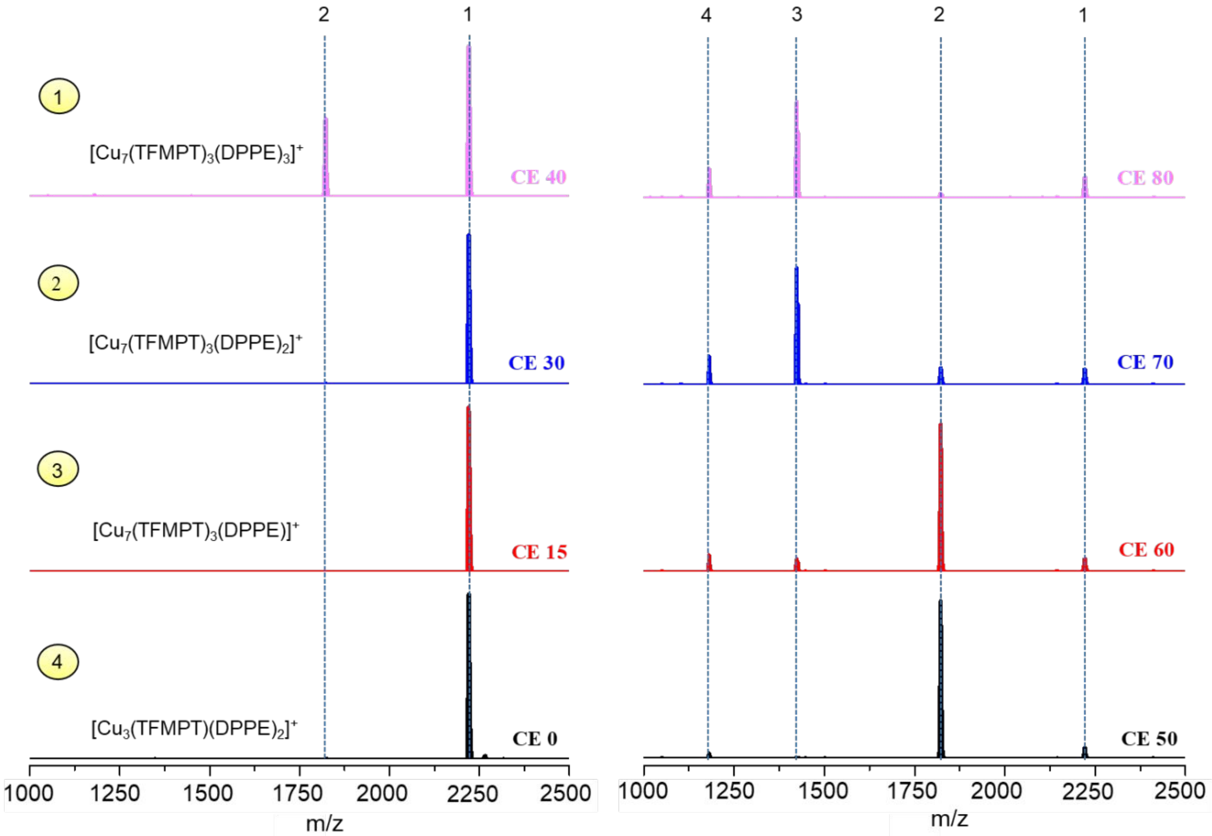

Figure S6. Collision energy dependent fragmentation of fragmented species. Inset shows molecular formula.

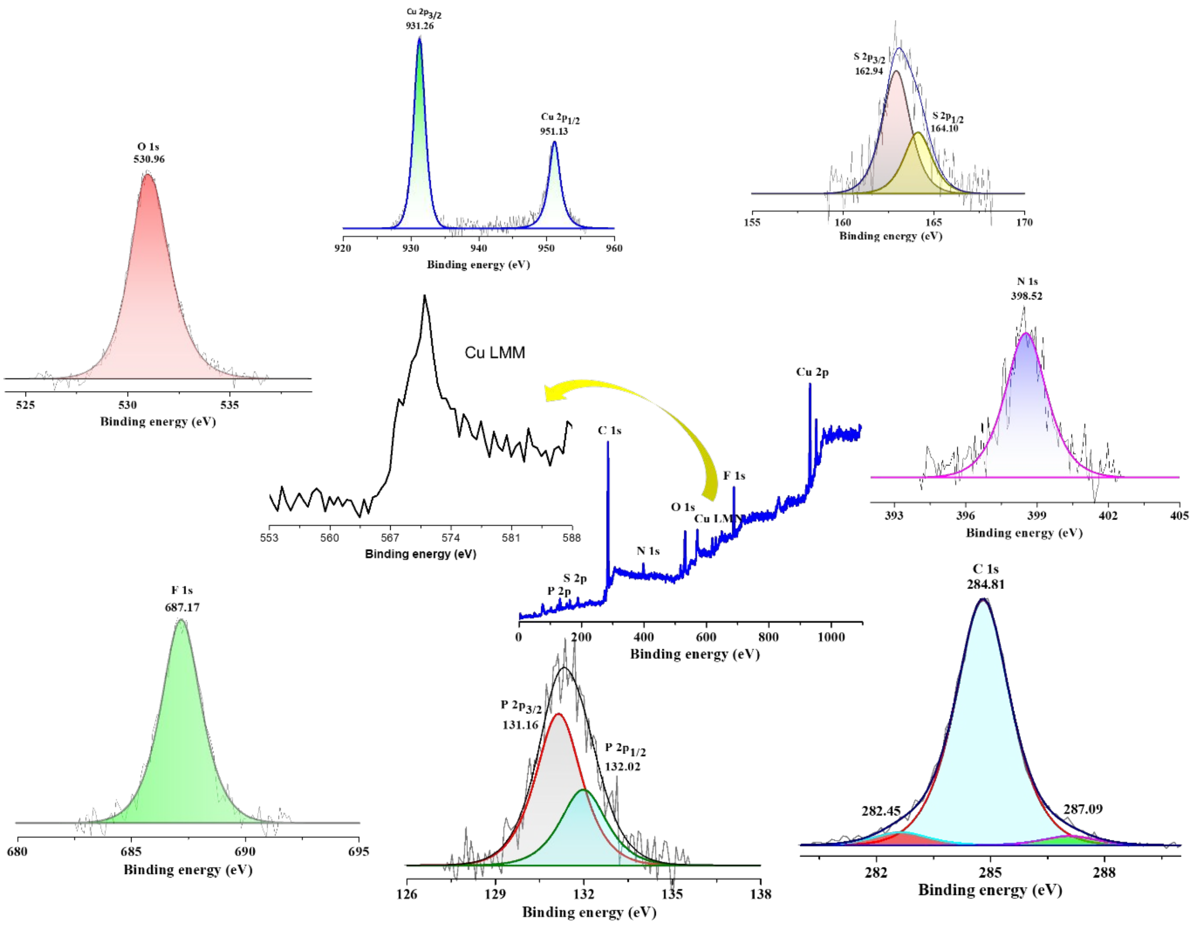

Figure S7. XPS survey spectra of singe crystals showing presence of respective elements. Expanded peak fittings of spectral region for each elements are shown. Inset shows Cu LMM auger spectral region.

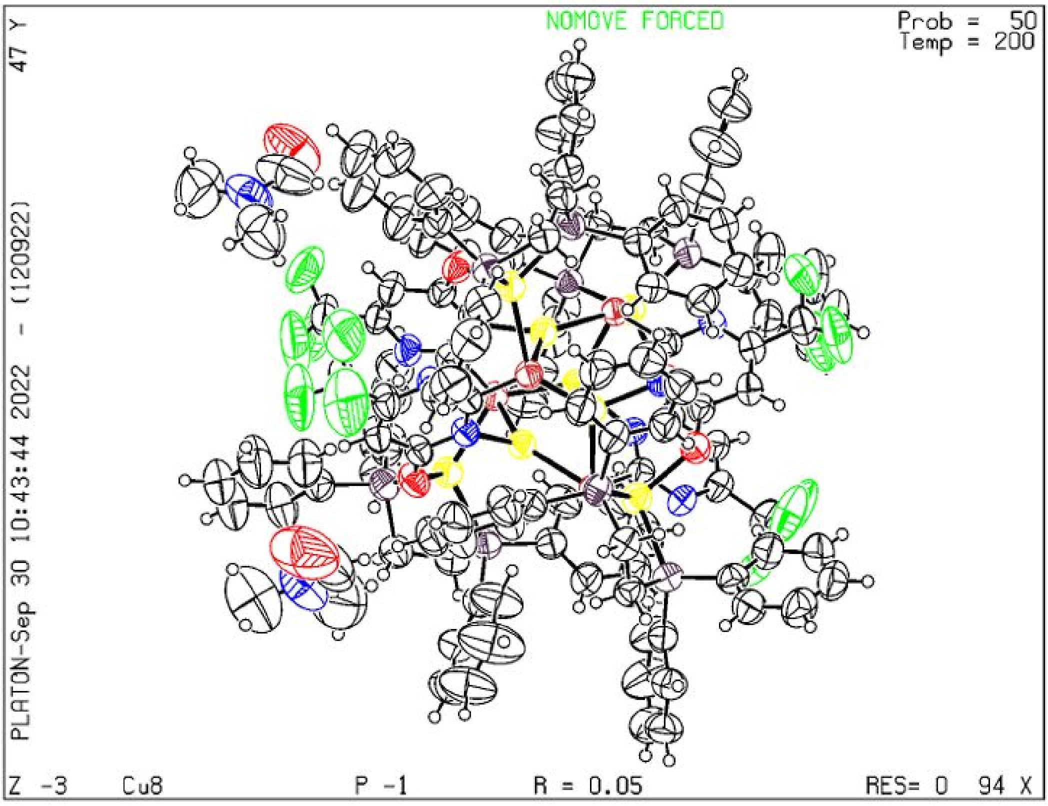

Figure S8. ORTEP structure of Cu_8 nanocluster with 50% thermal ellipsoid parameters.

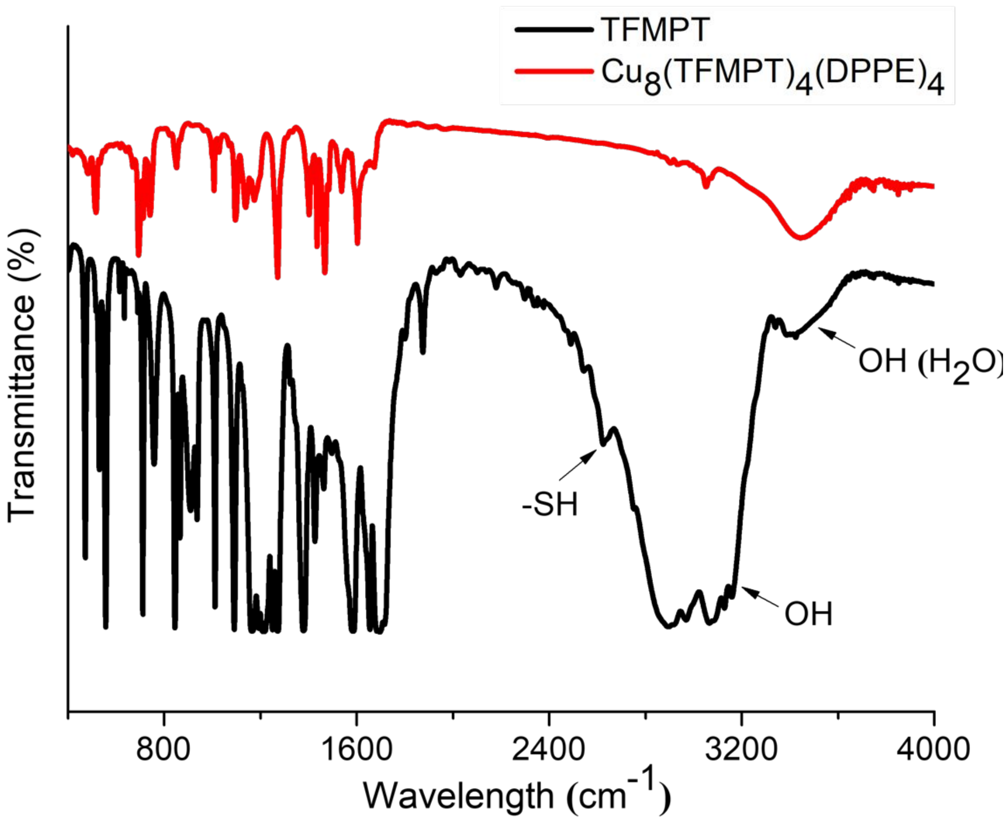

Figure S9. FTIR spectrum of Cu_8 NC in compared to the free ligand. Stretching vibrations are mentioned here.

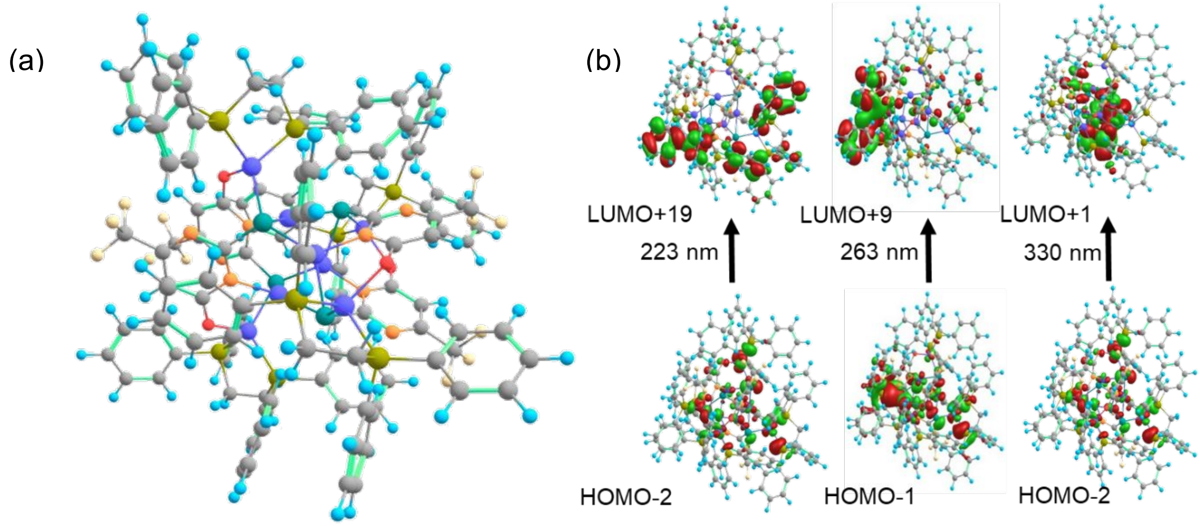

Figure S10. (a) DFT optimized structure of Cu_8. (b) Atomic color code: blue=Cu, green=S, grey=C,yellow=P, red=O, peaceful blue=N and bright blue=H.

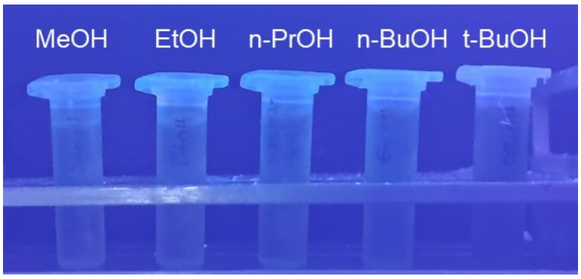

Figure S11. Volume fraction (80%) of polar protic solvents under UV light (365 nm) showing no emission from mixture.

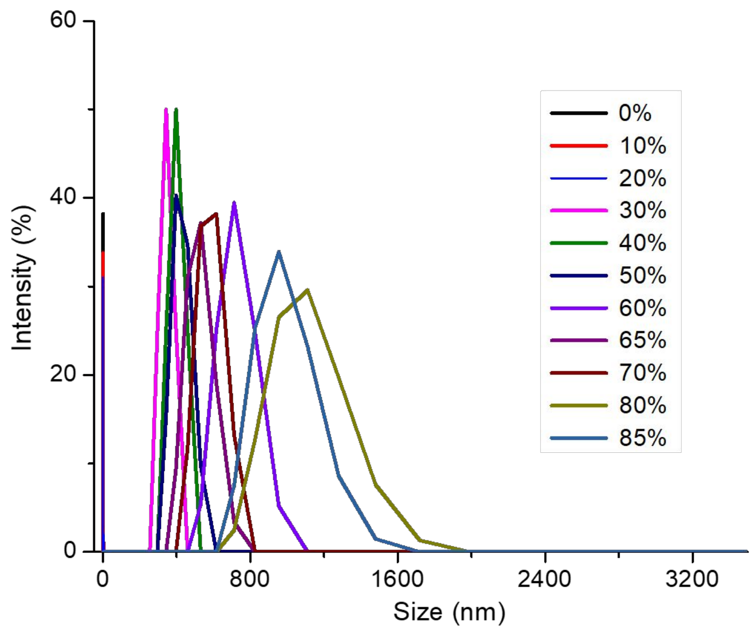

Figure S12. Dynamic Light Scattering (DLS) data of aggregated luminescent clusters with different vol% of water.

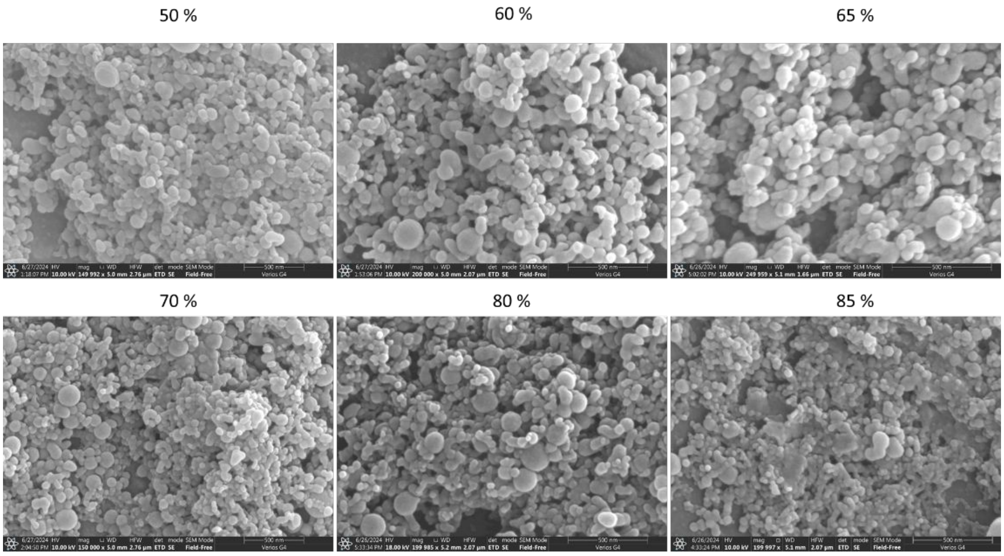

Figure S13. HRSEM images of clusters assembled spheroids at different vol% of water.

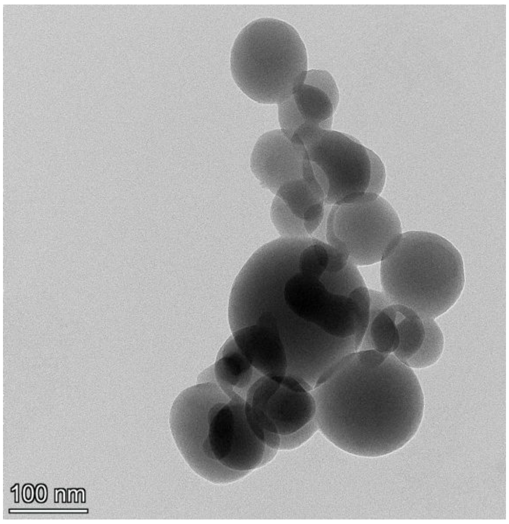

Figure S14. Transmission electron microscopy (TEM) image of spheroids (80% volume fraction of water) under 300 kV.

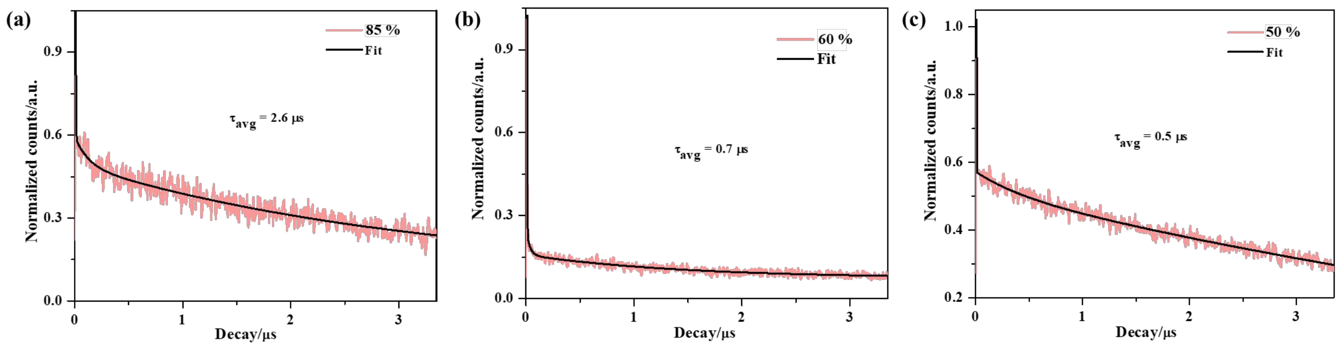

Figure S15. Lifetime decay profile of luminescent aggregates at different vol% of water (a) 85%, (b) 60% and (c) 50%. A deconvolution fit including the Instrument Response Function (IRF) of the laser diode (405 nm) was performed.

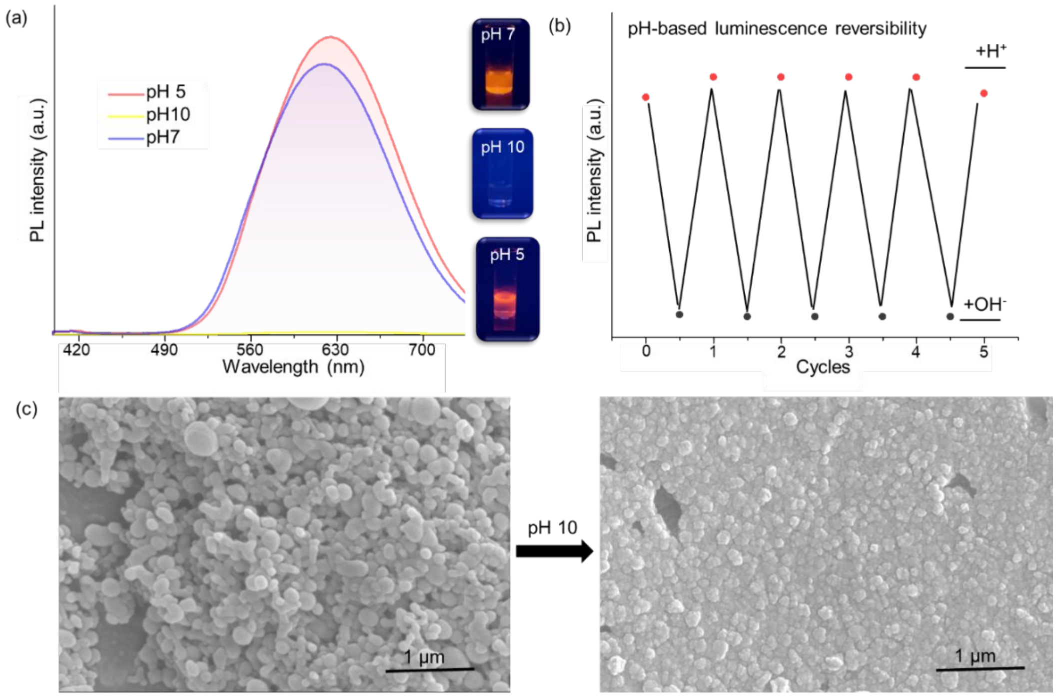

Figure S16. (a) pH-induced luminescence intensity change. (b) pH-based luminescence switching. (c) Surface morphology of spheroids upon change in pH from neutral to pH 10.

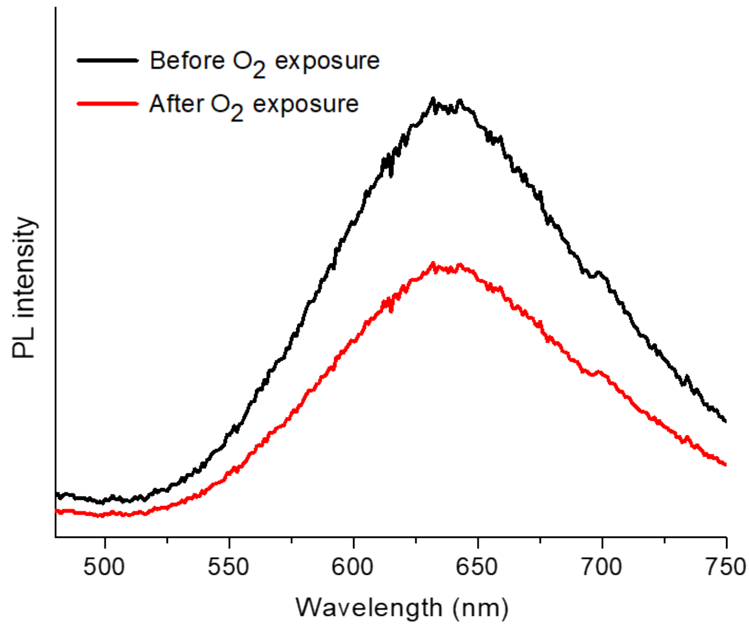

Figure S17. Comparative PL spectra of luminescent aggregates before and after oxygen exposure (Excitation at 365nm).

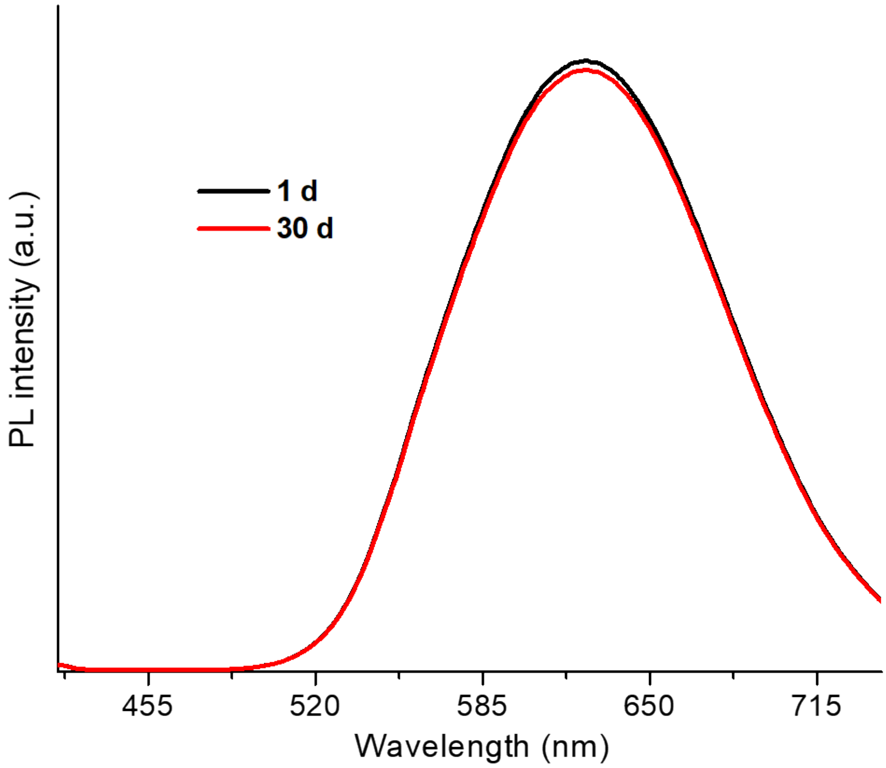

Figure S18. PL spectra for stability of luminescent aggregates, showed its ambient stability after 30 days (Excitation at 365 nm).

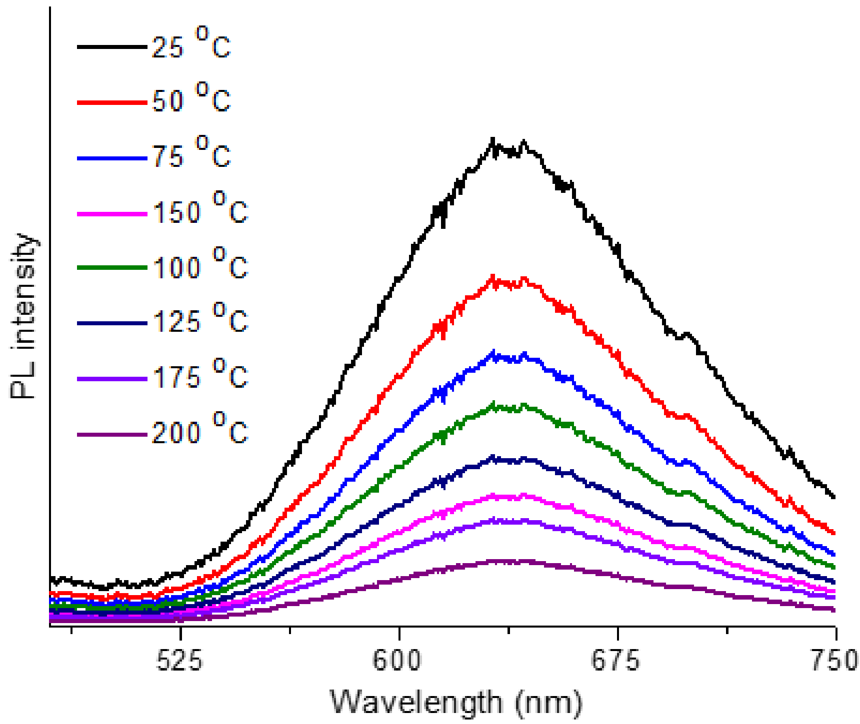

Figure S19. PL spectra of luminescent aggregates upon heating at different temperatures (Excitation at 365 nm and emission at 625 nm).

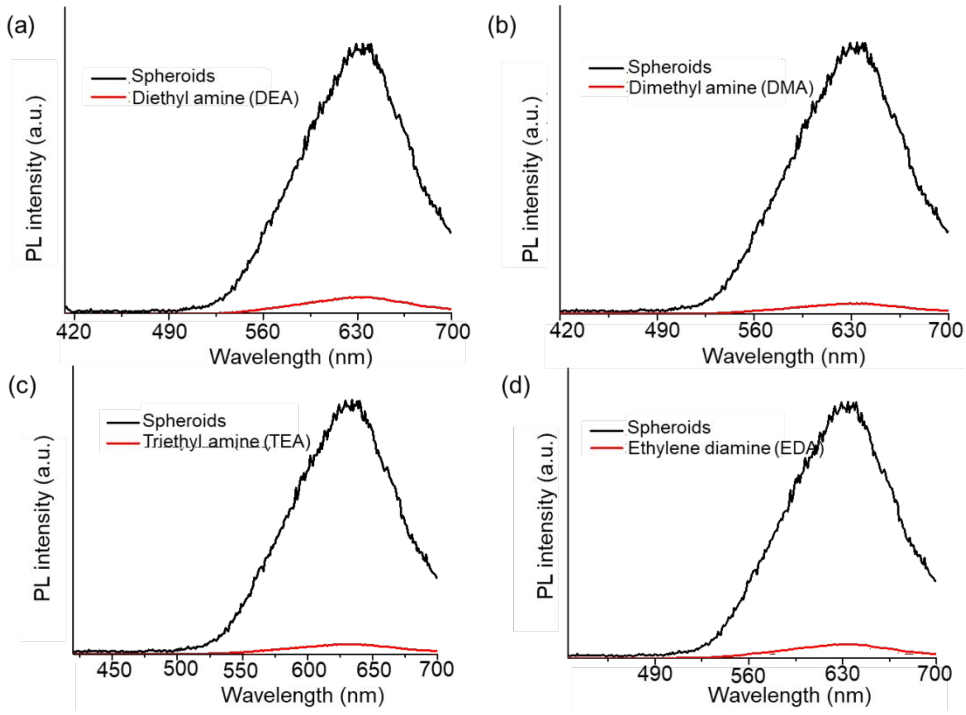

Figure S20. Comparative PL spectra of luminescent aggregates of Cu_8 clusters before and after the exposure to amine vapors (Excitation at 365 nm). Exposure time 12 mins.

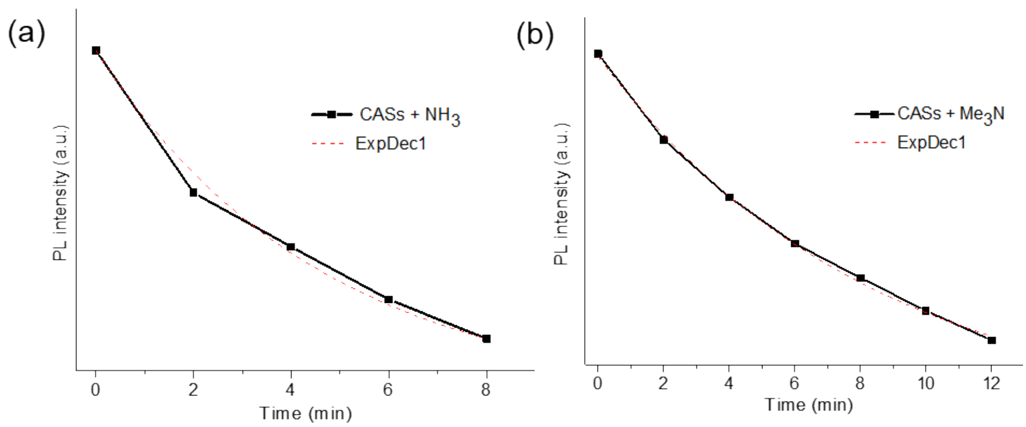

Figure S21. PL intensity change with time for (a) NH_3 and (b) NMe_3 respectively.

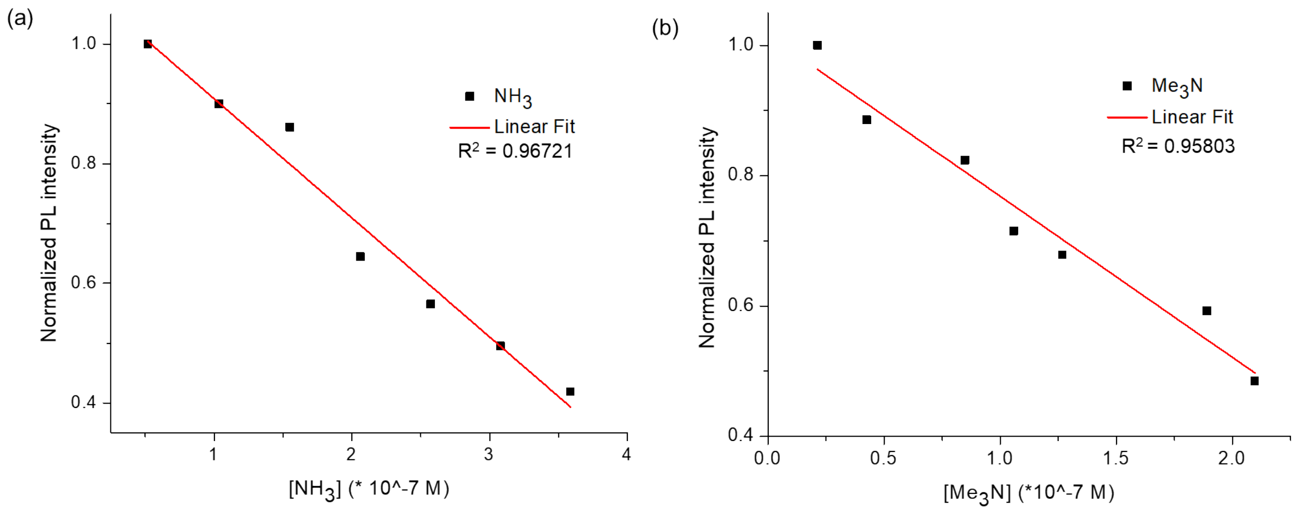

Figure S22. PL intensity change with concentration upon addition of (a) liquid NH_3 and (b) liquid NMe_3 to suspended aggregates in water respectively.

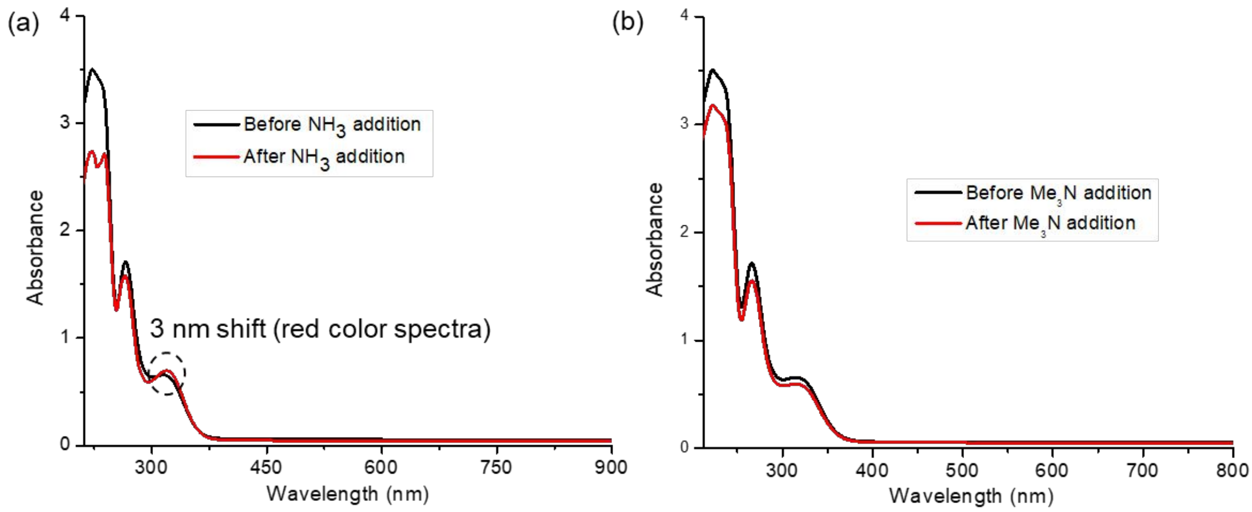

Figure 23. Stability check of cluster through UV-vis spectroscopy. (a) absorption spectra of solution before and after adding NH_3 to cluster-assembled luminescent aggregates. (b) absorption spectra of solution before and after adding Me_3N to cluster-assembled luminescent aggregates.

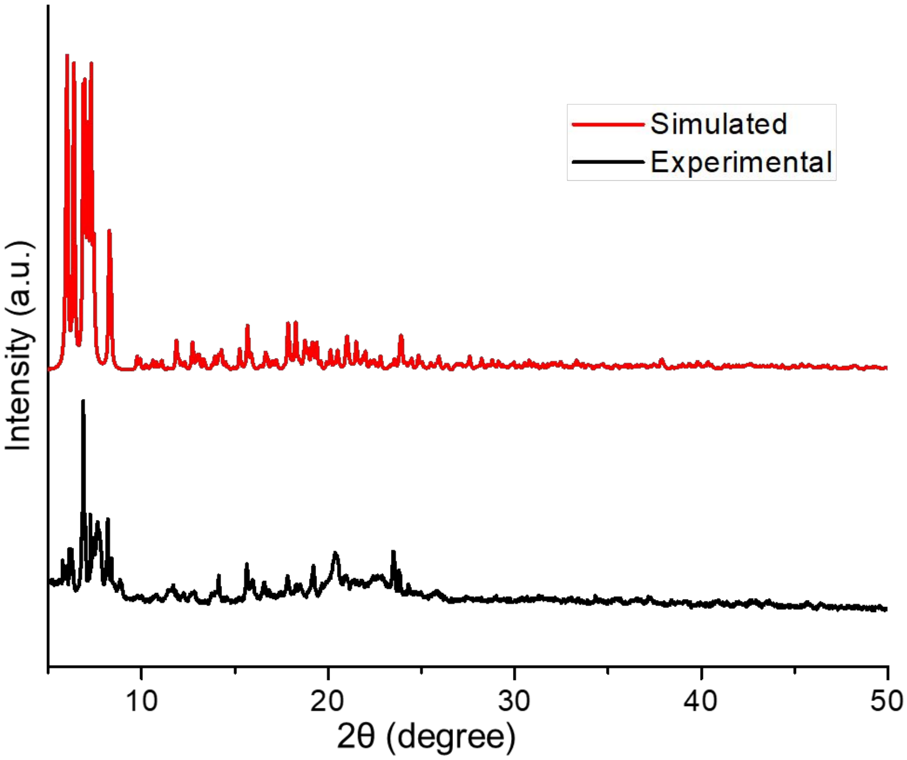

Figure S24. Comparative powder x-ray diffraction pattern of solid Cu_8 NC.

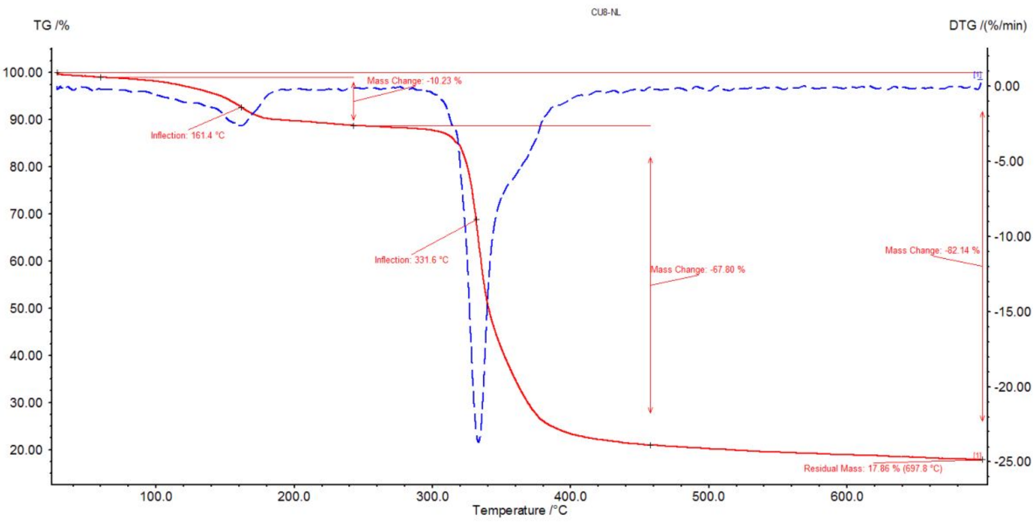

Figure S25. Thermogravimetry (TG) and derivative thermogravimetry (DTG) spectra of Cu_8 NC. Initial mass loss is possibly due to the evaporation of solvent molecules.

References

(1) Wang, Y.M.; Lin, X.C.; Mo, K.M.; Xie, M.; Huang, Y.L.; Ning, G.H.; Li, D. An Atomically Precise Pyrazolate-Protected Copper Nanocluster Exhibiting Exceptional Stability and Catalytic Activity. *Angew. Chem. Int. Ed.* **2023**, *62*(9), 202218369.

(2) Liao, P.K.; Sarkar, B.; Chang, H.W.; Wang, J.C.; Liu, C.W. Facile entrapment of a hydride inside the tetracapped tetrahedral Cu^I_8 cage inscribed in a S_{12} icosahedral framework. *Inorg. Chem.* **2009**, *48*(9), 4089-4097.

(3) Liu, L.J.; Wang, Z.Y.; Wang, Z.Y.; Wang, R.; Zang, S.Q.; Mak, T.C. Mediating CO_2 electroreduction activity and selectivity over atomically precise copper clusters. *Angew. Chem.* **2022**, *134*(35), 202205626.

(4) Sun, P.P.; Han, B.L.; Li, H.G.; Zhang, C.K.; Xin, X.; Dou, J.M.; Gao, Z.Y.; Sun, D. Real-Time Fluorescent Monitoring of Kinetically Controlled Supramolecular Self-Assembly of Atom-Precise Cu_8 Nanocluster. *Angew. Chem.* **2022**, *134*(20), 202200180.

(5) Xu, Y.; Dong, Q.G.; Dong, J.P.; Zhang, H.; Li, B.; Wang, R.; Zang, S.Q. Assembly of copper-clusters into a framework: enhancing the structural stability and photocatalytic HER performance. *Chem. Commun.* **2023**, *59*(21), 3067-3070.